Published in final edited form as:
Free Radic Res. 2011 February ; 45(2): 188–200. doi:10.3109/10715762.2010.522575.

Bioavailability of metalloporphyrin-based SOD mimics is greatly influenced by a single charge residing on a Mn site

Ivan Spasojevic[1], **Ivan Kos**[2,3], **Ludmil T. Benov**[4], **Zrinka Rajic**[2], **Diane Fels**[2], **Casey Dedeugd**[2], **Xiaodong Ye**[5], **Zeljko Vujaskovic**[2], **Julio S. Reboucas**[6], **Kam W. Leong**[5], **Mark W. Dewhirst**[2], and **Ines Batinic-Haberle**[2]

[1]Department of Medicine, Duke University Medical School, Durham, NC 27710, USA

[2]Department of Radiation Oncology, Duke University Medical School, Durham, NC 27710, USA

[3]Department of Analytical Chemistry, Faculty of Pharmacy and Biochemistry, University of Zagreb, 10000 Zagreb, Croatia

[4]Department of Biochemistry, Faculty of Medicine, Kuwait University, 13110 Safat, Kuwait

[5]Department of Biomedical Engineering, Duke University, Durham, NC 27708, USA

[6]Departamento de Química, CCEN, Universidade Federal da Paraíba, João Pessoa, PB 58051-970, Brazil

Abstract

In the cell Mn porphyrins (MnPs) likely couple with cellular reductants which results in a drop of total charge from 5+ to 4+ and dramatically increases their lipophilicity by up to three orders of magnitude depending upon the length of alkylpyridyl chains and type of isomer. The effects result from the interplay of solvation, lipophilicity and stericity. Impact of ascorbate on accumulation of MnPs was measured in *E. coli* and in Balb/C mouse tumours and muscle; for the latter measurements, the LC/ESI-MS/MS method was developed. Accumulation was significantly enhanced when MnPs were co-administered with ascorbate in both prokaryotic and eukaryotic systems. Further, MnTnHex-2-PyP^{5+} accumulates 5-fold more in the tumour than in a muscle. Such data increase our understanding of MnPs cellular and sub-cellular accumulation and remarkable *in vivo* effects. The work is in progress to understand how coupling of MnPs with ascorbate affects their mechanism of action, in particular with respect to cancer therapy.

Keywords

SOD mimics; peroxynitrite scavengers; Mn(III) N-alkylpyridyl porphyrins

Introduction

Mn(III) *N*-alkylpyridylporphyrins are among the most potent scavengers of superoxide (Table I) and peroxynitrite [1,2]. Besides, they are able to remove other reactive species such as $CO_3^{\cdot -}$, lipid peroxyl radicals, react with ·NO and judged by the activity of similar Mn porphyrins are likely able to efficiently remove HClO also [1,2].

Correspondence: Ivan Spasojevic, Department of Medicine, Duke University Medical Center, Durham, NC 27710, USA. Tel: 919-684-8311. Fax: 919-684-8380. spaso001@mc.duke.edu and Ines Batinic-Haberle, Department of Radiation Oncology, Duke University Medical Center, Durham, NC 27710, USA. Tel: 919-684-2101, Fax: 919-684-8718. ibatinic@duke.edu.

Declaration of interest

Reactive oxygen species (ROS) have been traditionally viewed as by-products of aerobic metabolism or a response to toxic stimuli. Often, superoxide is formed first, followed by a plethora of reactive species: hydrogen peroxide, hydroxyl radical, peroxynitrite, hypochlorus acid and singlet oxygen [3]. In order to cope with excess ROS, cells have a variety of redundant antioxidant defence systems: several superoxide dismutases, gluthatione peroxidases, glutathione reductases, catalase, a family of thioredoxins, peroxiredoxins, a family of glutathione S-transferases, glutaredoxins and others [4]. However, deliberate ROS production by a family of NADPH oxidases (NOX) plays an important role in the signalling pathways under both physiological and pathological conditions [5–8]. There are seven members of the NOX family: NOX1 through NOX5, which are generally considered to produce superoxide, and two hydrogen peroxide releasing DUOX1 and DUOX2 [5]. The first described, phagocytic NOX2, is activated during phagocytosis and produces high levels of superoxide [5]. In contrast, as a response to different stimuli, NOX 1, 3, 4 and 5 in non-phagocytic cells produce only small amounts of ROS, which act as second messengers in a wide variety of cells and under various conditions. NOX1 is expressed in colon epithelial and vascular smooth muscle cells, NOX3 in the inner ear, NOX4 in the kidney and NOX 5 in the testes and spleen [5]. Some of the known stimuli of the non-phagocytic NOX are angiotensin-II, thrombin, receptor tyrosine kinases, insulin, PDGF, bFGF, VEGF, angiopoietin and tumour necrosis factor receptor family [7]. In order to avoid collateral damage to biologically important molecules and cellular compartments, NOX mediated production of superoxide and subsequally ROS are regulated by mechanisms which control site, amount, duration and type of the ROS produced [6].

During tumour development, ROS not only cause genomic instability, which leads to tumour initiation and progression [9], but also activate cellular signalling pathways that, in turn, upregulate tumour proliferation, angiogenesis and metastasis [10]. Tumours can endure higher ROS levels, which would have triggered senescence and apoptosis in normal cells. Moreover, a tumour can utilize excessive oxidative burden to its advantage, i.e. for its progression [8]. Yet, at exceedingly high levels of ROS, tumour growth is suppressed or disabled [8]. Therefore, both antioxidants (that deplete tumour from signalling molecules) and pro-oxidants (that impose excessive oxidative burden upon the tumour) are being explored for the therapeutic potential as anti-cancer agents in the clinics [11].

By removing reactive species, Mn porphyrins decrease the consequences of primary oxidative stress by protecting biological molecules, but also finely tune redox-based cellular transcriptional activity and thus suppress excessive inflammatory and immune responses [12]. Consequently, they proved efficacious in reducing injuries of the central nervous system, radiation damage, diabetes-related disorders, as anticancer agents, etc. [1] and are therefore considered for clinical development. Most perspective candidates have been MnTE-2-PyP^{5+} (AEOL10113), MnTnHex-2-PyP^{5+} and MnTDE-2-ImP^{5+} (AEOL10150) [1]. The most lipophilic among them, MnTnHex-2-PyP^{5+}, appears up to 120-fold more efficacious than either of the other compounds (Figure 1) [1,2,12].

Although excessively hydrophilic, those pentacationic porphyrins are found in all tissues, cells and cellular compartments such as mitochondria [13] and nucleus [12].

Antioxidant potency

The ability to catalyze $O_2^{\cdot -}$ dismutation (log k_{cat} in Table I) best describes the antioxidant potency of the cationic Mn(III) *N*-alkylpyridylporphyrins [1,2]. The reason lies in the fact that the SOD-like activity parallels the $ONOO^-$ scavenging ability and, in turn, the ability of MnPs to finely tune cellular redox-based transcriptional activity [1,2,12,14]. We extensively addressed the antioxidant potency and accumulated a sufficient knowledge on the structure–activity relationship which allows us to accurately identify a drug candidate [1,12]. Due to

the ability to easily donate and accept electrons from redox-able biological molecules, MnPs can also produce a therapeutic effect via pro-oxidative mechanism [12,15,16]. Research is in progress to further understand such seemingly 'opposing' modes of action/s. In a two-step $O_2^{\cdot -}$ dismutation process, MnP acts both as pro- and anti-oxidant, oxidizing and reducing $O_2^{\cdot -}$. With efficacious MnP-based SOD mimics that dismute $O_2^{\cdot -}$ at around the potential of SOD enzymes, both processes occur with similar rate constants. Such data clearly suggest that Mn porphyrins may be equally good in acting as anti- and pro-oxidants in other *in vivo* systems also. These considerations are also reminiscent of anti- and pro-oxidative actions of MnSOD, which have been recently widely contemplated (see Discussion) [11,17].

Indeed, with high endogenous ascorbate levels, MnP may become oxidant and catalyze the oxygen consumption by ascorbate leading to excessive production of peroxide until ascorbate and/or oxygen is consumed [1,2,16,18–21]. We have already reported in a number of our publications the chemical evidence for the formation of peroxide in the presence of MnP and ascorbate [1,2,20,22] (see also in Discussion under Mechanism of action).

Bioavailibility of Mn porphyrins

The *in vivo* efficacy of MnPs is governed not only by their antioxidant potency, but also by their bioavailability. Recently, we have aimed at understanding which factors affect the bioavailability of Mn porphyrins and, in turn, their efficacy. The bioavailability is governed by lipophilicity, bulkiness, shape, charge, substituents and overall geometry of MnPs. MnP lipophilicity by itself is a fair measure of porphyrin bioavailability [23–25] and has been characterized by either chromatographic retention factor R_f [1,2] or partition of Mn porphyrin between n-octanol and water, log P_{OW} [26]. R_f and log P_{OW} for Mn(III) *N*-alkylpyridylporphyrins are linearly related. The determination of R_f is much simpler relative to log P_{OW}; in some cases log P_{OW} can not be even determined due to excessive hydrophilic character of some MnPs. The log P_{OW} can be accurately obtained from R_f vs log P_{OW} linear dependence [26]. Few studies showed that Mn porphyrin must possess both fair antioxidant potency and appropriate lipophilicity to be efficacious *in vivo* [23–26]. The recent comprehensive *E. coli* study [25] most clearly showed the vast impact of MnP lipophilicity on its efficacy. The series of isomeric *ortho* and *meta* isomers (Figure 1) was studied with respect to their cellular accumulation and ability to allow SOD-deficient *E. coli* to grow aerobically as the wild type. The *meta* MnTE-3-PyP^{5+} is ~10-fold less SOD-active, but is 10 fold more lipophilic and accumulated 10-fold more in *E. coli* than *ortho* MnTE-2-PyP^{5+}. Its higher accumulation fully compensates for inferior SOD-like activity. Consequently, under the same conditions, MnTE-2-PyP^{5+} and MnTE-3-PyP^{5+} were equally able to compensate for the lack of cytosolic superoxide dismutases.

The present study explores the effect of charges on Mn porphyrins lipophilicity and, consequently, on their cellular accumulation. Due to favourable, highly positive $E_{1/2}$ (Table I), the cationic *ortho* Mn(III) *N*-alkylpyridylporphyrins are readily reduced by ascorbate, glutathione, tetrahydrobiopterin and flavoenzymes [2,12,17,27–30]. As the cellular levels of ascorbate and glutathione are high [4], those MnPs would likely be reduced inside the cell. Evidence that this is indeed true was already reported with *E. coli* [25,31]. Upon reduction, the total charge drops from 5+ to 4+, whereby the single charge at the Mn centre is lost. Since the peripheral charges remain the same, no major impact of charge reduction on lipophilicity has been anticipated. Surprisingly, upon reduction, the MnP lipophilicity increased as much as 850-fold, which has a significant impact on the porphyrin accumulation both in prokaryotic *E. coli* cell and in eukaryotic mouse tumour and muscle. For comparison, the analogous *meta* isomer, MnTM-3-PyP^{5+} was also explored. Such data further our insight into the remarkable *in vivo* efficacy of *ortho* isomeric Mn porphyrins, their accumulation in mitochondria and in central nervous system (which is rich in ascorbate) and support their clinical development.

Materials and methods

Materials

Mn porphyrins were synthesized as previously described [2,22,25,26,32]. Acetonitrile was from Fisher Scientific. Plastic-backed silica gel TLC plates (Z122777-25EA), sodium ascorbate and KNO_3 were purchased from Sigma-Aldrich. Sodium dithionite was from J. T. Baker.

Thin-layer chromatography

Thin-layer chromatography of Mn porhyrins was performed on silica gel TLC plates (plastic-backed) with KNO_3-saturated H_2O:H_2O:acetonitrile = 1:1:8 mixture as a mobile phase. Typically, 1 μL of ~1 mM samples was applied at ~1 cm of the strip border and the solvent front was allowed to run ~8 cm. The 1 mM *ortho* porphyrins were reduced with 20 mM ascorbate; ~5 min were allowed for complete reduction. Less reducible MnPs of *meta* series (see $E_{1/2}$ values in Table I) were reduced with a much stronger reducing reagent, sodium dithionite. Aerobically, ascorbate reduces MnTM-3-PyP^{5+} slowly and incompletely. Upon addition of sodium dithionite the MnP was immediately placed on a silica plate. Longer exposure to such strong reductant leads to the reduction of porphyrin ring with its subsequent decomposition observed as the decolouration of solution. The R_f values are sensitive to the degree of the saturation of vapour phase in the TLC chamber and may differ slightly from one to another experiment. Thus, the internal standardization of TLC, using MnTE-2-PyP^{5+}, is required for comparison purposes [33]*. Experimental determination of log P_{OW} for the reduced porphyrins is not possible, as ascorbate is hydrophilic and can not be extracted into n-octanol with porphyrin. Without ascorbate Mn^{II}Ps are not stable and can not be isolated. Therefore, log P_{OW} of the reduced MnPs was calculated from experimentally determined R_f according to equations: log $P_{OW} = 12.18 \cdot R_f - 7.43$ (*ortho* porphyrins) and log $P_{OW} = 8.78 \cdot R_f - 7.12$ (*meta* porphyrins) (Table II) [26]. Calculation of log P_{OW} from the equation log P_{OW} vs nC in the case of the reduced MnPs is not possible, because that equation takes into account only the number of carbon atoms regardless of the Mn centre redox state. In the series of oxidized MnPs, differences in calculated log P_{OW} values by both equations are negligible, except for Mn^{III}TM-2-PyP^{5+} and Mn^{III}TE-3-PyP^{5+}.

In order to gain further insight into the lipophilicity of 4+-carrying ions, we performed TLC under identical conditions for Mn^{III}TE-2-PyP^{5+} and for tetracationic species: Mn^{II}TE-2-PyP^{4+}, metal-free ligand, H_2TE-2-PyP^{5+} [22] and its Zn complex, ZnTE-2-PyP^{4+}. ZnP was synthesized as previously described [2]. Mn^{III}TE-2-PyP^{5+} was reduced with ascorbate; thus TLC of Mn^{II}TE-2-PyP^{4+} is the only one out of compounds tested to have excess ascorbate in solution. Ascorbate may also act as counterion replacing chloride and/or nitrate ions (the latter coming from excess KNO_3 in TLC solvent mixture) and affect R_f value. To account for the effect of ascorbate, the TLC was done with H_2TE-2-PyP^{4+} and ZnTE-2-PyP^{4+} solutions prepared with and without ascorbate. There was no effect of ascorbate on R_f.

Accumulation of Mn porphyrins in E. coli

A wild type *Escherichia coli* strain AB1157 was used in this study (*F-thr-1*; *leuB6*; *proA2*; *his-4*; *thi-1*; *argE2*; *lacY1*; *galK2*; *rpsL*; *supE44*; *ara-14*; *xyl-15*; *mtl-1*; *tsx-33*) [34]. The experiments were carried out in triplicate, as described in detail in Batinić-Haberle et al. [35]. The accumulation experiment was performed with wild type AB1157 since it grows faster. Deionized water was used throughout the study. The *E. coli* was grown in flasks in 10 mL of casamino M9CA medium to a density corresponding to A_{700} ~0.6. Then 5 μM Mn

*The best approach would be to run in parallel TLC of all compounds of interest.

porphyrins alone were added in one experiment and together with 0.5 or 1 mM sodium ascorbate in another one. The cells were kept on a shaker for an additional 60 min. Cells were then rapidly washed with ice-cold PBS, resuspended to a total volume of 1.0 mL and disrupted by sonication. Cytosolic and cell wall fractions were separated by centrifugation. Cell walls are minor fraction of the cell. Due to insufficient material, the quantification of Mn porphyrins is less reliable in cell walls than in cytosols. Spectra were recorded and the absorbances of MnPs measured at their Soret bands [2]. Protein levels were measured by Lowry method [36]. In the growing medium, under aerobic conditions and in the absence of reductants, MnPs are stabilized with Mn being in +3 oxidation state. Due to the reductive cellular environment and particularly when *E. coli* was growing in the presence of ascorbate, inside the respiring cell MnPs exist predominantly as Mn^{II}Ps. However, it is close to impossible to prevent the oxidation of Mn^{II}P to Mn^{III}P during manipulation of the cells and thus to assess unambiguously the oxidation state of Mn within intact cells. Even after cell disruption, the spectra of processed cytosolic fractions still showed significant levels of reduced Mn^{II}P, which suggests extensive reduction of MnP within the respiring cell. Two maxima were seen, one related to oxidized Mn^{III}P at ~454 nm for *ortho* and at 460 nm for *meta* isomers, the other related to reduced Mn^{II}P at shorter wavelengths of ~440 nm. Upon centrifuging the casamino M9CA medium containing cells and before any manipulation, the cellular pellet was greenish, which is a clear sign of the presence of porphyrin in a reduced state, Mn^{II}P (oxidized Mn^{III}P is brown-reddish). Two approaches were adopted to calculate the levels of MnPs in cytosolic fractions: (a) using the molar absorptivities and (b) using area below the Soret band. For the latter, the calibration curve was constructed where the area below the Soret band was plotted vs concentration of either *ortho* or *meta* porphyrins [25]. Both approaches offered the same conclusions, but the latter appeared to be a more correct strategy as it accounted for both oxidized and reduced porphyrin.

Tumour and muscle levels of MnTnHex-2-PyP^{5+}

The tumours and muscle, provided from a 4T1 breast cancer mouse study (publication in preparation, few data available in refs [1] and [16]) were used to determine the levels of Mn porphyrins. All *in vivo* procedures were conducted in accordance with a protocol approved by the Duke University Institutional Animal Care and Use Committee. Four groups of Balb/C female mice weighing on average 20 g with 15 mice per group were studied: (1) 400 μL of PBS ip; (2) sodium ascorbate 2 g/kg twice daily ip; (3) MnTnHex-2-PyP^{5+} 1 mg/kg twice daily sc; (4) MnTnHex-2-PyP^{5+} 1 mg/kg twice daily sc and sodium ascorbate 2 g/kg twice daily ip. In the 4th group, sodium ascorbate was delivered 1 h after the injection of MnTnHex-2-PyP^{5+}. Tumours were established from a 100 μL single cell suspension of 1 × 10^6 cells/mL injected subcutaneously into the right flank of mice. The doses of MnP and ascorbate chosen were based on *in vivo* experiments [37,38]. Mice were sacrificed 12 h after the last drug injection and tumours and the normal muscle from the non-tumour bearing leg were excised for MnP analysis. Given the data from pharmacokinetic studies [39], 12 h after the injection of the drug, no significant levels are supposed to be in the blood. Thus, blood content did not affect MnP tumour and muscle levels.

LC/ESI-MS/MS analysis

Tumours and muscles were homogenized (1/3 g tissue/mL water), proteins removed from tissue with 1% acetic acid in methanol (1/2 homogenate/methanol), solvent evaporated and residue reconstituted in mobile phase A (see below). Analyses were performed at Duke Comprehensive Cancer Center, Clinical Pharmacology Laboratory.

LC conditions—Shimadzu 20A series HPLC; column: Phenomenex 4 × 3 mm, C_{18} guard cartridge only; column temperature: 35 °C; mobile phase A: 95:5 H_2O:acetonitrile (0.1% heptafluorobutyric acid, HFBA); mobile phase B: acetonitrile (0.1%, HFBA); elution

gradient: 0–0.2 min, 0–90% B, 0.2–0.7 min, 90% B, 0.7–0.75 min, 90–0% B; run time: 4 min; injection volume: 10 μL.

MS/MS conditions—Applied Biosystems MDS Sciex 3200 Q Trap or 4000 Q Trap ESI-MS/MS; MRM transitions: MnTnHex-2-PyP^{5+} at m/z 825.5/611.5 (parent ion [MnP^{5+} + 3HFBA^{-}]$^{2+}$/2) and MnTnHep-2-PyP^{5+} (internal standard) at m/z 853.5/639.5. Calibration samples in 0.1–30 μM range were prepared by adding known amounts of MnTnHex-2-PyP^{5+} into homogenates of tumours and muscles of untreated mice and were run along with study samples. Linear response was observed in the concentration range measured.

Results and discussion

Ascorbic acid

Along with glutathione, ascorbate is our main endogenous low molecular-weight antioxidant. Its major role is to assure the action of α-tocopherol in preventing lipid peroxidation (via reduction of α-tocopherol radical back to α-tocopherol) and, thus, in turn, maintains the cell membrane integrity. After intestinal apsorption, ascorbate reaches plasma concentrations of 40–60 μM. The highest levels are found in the brain (2–4 mM) and adrenal gland (10 mM), where there is an abundance of lipids and α-tocopherol protection is critical. Concentration of ascorbate in the liver is 0.8–1 mM and in the muscle 0.4 mM [40–42]. Ascorbate cellular concentrations are up to two orders of magnitude higher than plasma levels.

Mn porphyrins

In vivo, due to easy reducibility of *ortho* isomeric Mn porphyrins (Table I), and significantly higher cellular levels of small molecular-weight endogenous antioxidants (mM levels [4]) than of the reactive species (nM to μM [4]), MnPs would readily couple with cellular reductants while removing $O_2^{\cdot -}$ and peroxynitrite. Upon reduction from Mn^{III}P to Mn^{II}P, they would reduce $O_2^{\cdot -}$ or $ONOO^-$ in a subsequent step. Such removal of $O_2^{\cdot -}$ is reminiscent of the action of superoxide reductase, such as rubredoxin oxidoreductase (desulphoferrodoxin) [43]. The reduction of $ONOO^-$ with Mn^{II}P may happen one- or two-electronically, leading to the production of $^{\cdot}NO_2$ radical or benign nitrite, NO_2^-, respectively [44].

Mn porphyrins + ascorbate

Reduction of *ortho* Mn porphyrins is involved not only in the elimination of reactive species, but may seemingly affect their cellular accumulation. Upon reduction of MnP with ascorbate, its charge drops for only one unit, from 5+ to 4+. The single charge gets lost from the Mn centre. Since peripheral charges remain unchanged, we expected no major impact of such charge reduction on lipophilicity. Surprisingly, the lipophilicity increased as much as 850-fold, depending upon the length of the alkyl chain and the type of the isomer (Table II).

The reduction of less reducible *meta* MnTM-3-PyP^{5+} (more negative $E_{1/2}$, Table I) was performed with sodium dithionite.

The log P_{OW} vs R_f

We previously showed that log P_{OW} of the oxidized Mn^{III}P is linearly related to the chromatographic R_f value [26]. Log P_{OW} of the reduced Mn^{II}P can not be experimentally assessed (see under Experimental). Thus, it was calculated from the R_f using reported equations and tabulated (Table II) [26]. R_f is much easier to determine and thus we use it to conveniently and routinely characterize the lipophilicity of Mn porphyrins [26].

The R_f vs alkyl chain length

We previously showed that lipophilicity of *ortho* and *meta* $Mn^{III}Ps$ increases as the *N*-alkylpyridyl chains lengthen from methyl to octyl in a linear fashion [26]. Herein we showed that this relationship is valid for both oxidized $Mn^{III}P$ and reduced $Mn^{II}P$ porphyrins and for both *ortho* and *meta* isomers (Figure 2). Figure 2, however, shows that as the alkyl chains lengthen beyond hexyl, the effect of the Mn site solvation (degree of which determines porphyrin hydrophilicity/lipophilicity) becomes increasingly suppressed and the porphyrin may eventually cease to sense whether the single charge resides on Mn or not. With short methyl chains the difference in lipophilicity between $Mn^{III}P$ and $Mn^{II}P$ is also smaller. There is seemingly an optimal length of alkyl chains that is critical for the creation of cavity which can support substantial MnP solvation.

Data in Figure 2 further show that the *meta* isomers are less sensitive to the loss of a single charge than *ortho* porphyrins (see discussion in next paragraph). To note, small differences in R_f values in Figure 2 correspond to large differences in log P_{OW} values (Table II) [26].

MnP reduction-based gain in lipophilicity as a function of alkyl chain length and type of isomer

We have further observed that the change in the lipophilicity upon MnP reduction is related to the length of alkyl chains and the type of the isomer. This relationship has a bell shape (Figure 3). Upon reduction, the change in lipophilicity of MnPs first increases as the alkyl chain lengthens up to butyl, but then decreases as the alkyl chain grows further (Figure 3). The effect is the consequence of the interplay of MnP lipophilicity, solvation and steric effects. As the chains lengthen from methyl to butyl, the cavity they form around the metal site gets larger and facilitates the Mn site solvation. When the chain lengthens beyond butyl, the impact of long lipophilic alkyl chains prevails, shielding the solvation effects arising from the single charge residing on a Mn site. A 17-fold stronger effect was observed with *ortho* than with *meta* isomers: with *meta* isomers the lipophilicity changes upon reduction by up to ~50-fold and with *ortho* by up to ~850-fold (Table II). The largest change in lipophilicity was observed with *ortho* and *meta* butyl compounds, MnTnBu-2(or 3)-PyP^{5+}. The difference between the gain in lipophilicity of *ortho* and *meta* isomers fades away as the chains become shorter. Small substituents, such as methyl groups, hardly create any cavity that would have enhanced metal centre solvation differently with *ortho* than with *meta* isomers.

Due to sterical crowding between alkyl chains and β-pyrrolic hydrogens of *ortho* porphyrin, the alkyl chains are fixed above and below the porphyrin plane and they define the cavity within which counterion and/or solvent molecules reside in a first and second Mn co-ordination sphere. With the *meta* isomer, there is no sterical hindrance; consequently, the alkyl chains freely rotate around pyridyl groups. Further, as the electron-withdrawing cationic pyridyl nitrogens are placed further away from the porphyrin core, the *meta* Mn(III) centre is more electron rich than the *ortho* Mn(III) site (see $E_{1/2}$ in Table I) and thus does not favour axial ligation and solvation as much as does the *ortho* analogue. The differences in electron richness/deficiency of isomers, which defines the solvation of the Mn site, are clearly seen in their mass spectra (MS) [46]. The major ions in the MS of *ortho* $MnT^{III}M$-2-PyP^{5+} have one or two chlorides axially bound to oxidized or reduced Mn site, while insignificant contribution of ions bearing two chlorides was found in the MS of *meta*, $MnT^{III}M$-3-PyP^{5+}. For such reasons: (1) the oxidized *ortho* Mn(III) *N*-alkylpyridylporphyrins are 10-fold more hydrophilic than are the *meta* species; (2) the *ortho* isomers on average sense 10-fold more the loss of single charge than do the *meta* analogues.

Lipophilicity of pentactionic Mn^{III}TE-2-PyP^{5+} vs different tetracationic species: Mn^{II}TE-2-PyP^{4+}, ZnTE-2-PyP^{4+}, H_2TE-2-PyP^{4+}

The effect of the metal site or the lack of it on MnP lipophilicity was clearly seen when pentacationic Mn^{III}TE-2-PyP^{5+} was compared to tetracationic Mn^{II}TE-2-PyP^{4+}, H^2TE-2-PyP^{4+} and ZnTE-2-PyP^{4+}. During redox cycling Mn^{II}TE-2-PyP^{4+} is formed, which is much less stable than Mn^{III}TE-2-PyP^{5+} and may lose metal to some extent whereby metal-free ligand would emerge. All tetracationic porphyrins, as expected, were more lipophilic than pentacationic, Mn^{III}TE-2-PyP^{5+}. The most lipophilic is the reduced Mn^{II}TE-2-PyP^{4+}, followed by Zn^{II}TE-2-PyP^{4+}. Out of tetracationic species, the metal-free ligand, H_2TE-2-PyP^{4+} appears the most solvated compound (Figure 4).

To further the insight into the effect of lipophilicity upon cellular accumulation we studied two *in vivo* models: prokaryotic *E. coli* and eukaryotic mouse. In plasma and in *E. coli* growing medium, MnPs presumably exist predominantly in their oxidized Mn(III) form. The concentration of ascorbate in the plasma of mammals is lower than in the cell and there is none in the cellular medium where prokaryotic *E. coli* grows. We aimed here to see if co-administration of ascorbate with porphyrins would enhance their *in vivo* accumulation, due to the gain in lipophilicity upon Mn^{III}P to Mn^{II} P reduction.

E. coli study

We were able to significantly enhance the accumulation of *ortho* MnPs within *E. coli*, when ascorbate was present in the growing medium. Yet, with the less reducible *meta* isomer MnTM-3-PyP^{5+}, no effect was observed (Figure 5). This is consistent with the data on equally reducible *para* isomer, MnTM-4-PyP^{5+}. The $E_{1/2}$ of MnTM-4-PyP^{5+} is +60 mV vs NHE while of MnTM-3-PyP^{5+} is +52 mV vs NHE. In a study on submitochondrial particles, MnTM-4-PyP^{5+} was not readily reduced with components of mitochondrial respiration [27]. A 130% enhancement of MnP accumulation by ascorbate was observed with *ortho* ethyl porphyrin, MnTE-2-PyP^{5+} (Figure 5, Inset).

Mouse study

In addition to *E. coli*, we also analysed the distribution of MnTnHex-2-PyP^{5+} in a mouse tumour and a muscle after 2 weeks of daily administration of MnP alone and along with ascorbate (Figure 6 and Table III). Two sets of observations were made: (1) MnTnHex-2-PyP^{5+} accumulates ~5-fold more in tumour than in muscle when administered either alone or with ascorbate; (2) Regardless of the type of tissue, ascorbate enhances MnP accumulation and does so to a similar extent: ~33% [(2.20–1.65)/1.65] in tumour and 54% [(0.48–0.31)/0.31] in muscle (Table III and Figure 6). Higher tumour accumulation of MnP may be due to leaky tumour vasculature [47] and to other effects discussed under *Accumulation of MnPs in tumour*.

A new LC/ESI-MS/MS method was developed for the determination of MnTnHex-2-PyP^{5+} in tumours and muscle tissue. It is less time- and labour-consuming than the HPLC/fluorescence method that we previously employed [13,38,39]. The HPLC/fluorescence method involves the Mn^{III}P reduction with ascorbate, followed by Mn to Zn exchange and ZnP fluorescence detection. With longer alkyl chain analogues, such as hexyl, it is nearly impossible to fully reduce MnP in order to exchange Mn for Zn. Thus, the LC/ESI-MS/MS method has wider applicability and, importantly, higher sensitivity where as low as 1 nM levels of MnPs in tissue homogenates may be measured.

The in vivo implications of MnP reduction-based enhancement in lipophilicity

It appears that the same factors that provide *ortho* isomers with high antioxidant potency and determine their mechanism/s of action—electron-deficiency, cationic charge next to the

metal site—also provide them with high gain in lipophilicity upon their reduction (the step that is a part of their catalytic antioxidant-based action) and thus favourably affect their tissue and sub-cellular accumulation.

Transport across the plasma membrane—We are assuming that in plasma at physiological concentrations of endogenous ascorbate, the Mn porphyrins are in (oxidized) +3 Mn oxidation state. The following calculation supports such speculation. If the blood volume of a 20 g mouse is 1.6 mL [48], then plasma concentration of MnTnHex-2-PyP^{5+} (given in a dose of 2 mg/kg daily) would be in the range of 10–62.5 μM. The first number is based on the mouse pharmacokinetic study of MnTE-2-PyP^{5+} [39] where 16% of the injected amount of 1 mg/kg reaches plasma. The second number (of 100% resorption) was based on 13500-fold higher lipophilicity of MnTnHex-2-PyP^{5+} which in turn suggests much higher blood levels. Ascorbate mouse plasma concentration of 42 μM (0.83 mg/100 mL) [49] is similar to a human plasma level of 40–60 μM [40,41]) and similar to MnP plasma concentration. Our previous data show that 1:1 ratio of ascorbate:MnP is insufficient to reduce MnP aerobically [22]; routinely we need 20-fold excess of ascorbate over MnP [22]. With a dose of 2 g/kg, ascorbate mouse plasma concentration reaches 126 mM; > 2000-fold excess of ascorbate, which ensures the reduction of Mn^{3+} to Mn^{2+} and, in turn, increases the MnP lipophilicity and facilitates the transport across the plasma membrane.

Accumulation of MnPs within mitochondria—Within the cell, regardless of the exogenous ascorbate, the abundance of endogenous ascorbate and other cellular reductants stabilize MnP in its reduced state. It is well accepted now that positive charge and lipophilicity drive compounds to the mitochondria [13,50]. A skin carcinogenesis study [51] indicated that MnTE-2-PyP^{5+} mimics MnSOD and suggests its likely accumulation in the mitochondrial matrix. The following study on submitochondrial particles indicated that MnTE-2-PyP^{5+} gets reduced by components of the mitochondrial respiratory chain to MnTE-2-PyP^{4+} which in turn scavenges $ONOO^-$ [27]. Thus, MnTE-2-PyP^{4+} binds $ONOO^-$ in a first step and reduces it to innocent NO_2^- in a subsequent step [18]. The mouse study, which followed, showed that indeed MnTE-2-PyP^{5+} accumulates in mouse heart mitochondria and at levels enough to protect it against $ONOO^-$-mediated damage [1,2,13,27]. The accumulation is greatly affected by MnP lipophilicity and is correlated with the alkyl-chain length; MnTnHex-2-PyP^{5+} accumulates significantly more in mitochondria relative to cytosol than MnTE-2-PyP^{5+} (Spasojevic, St Clair et al. unpublished). Such data correlate well with yeast mitochondria study on Mn(III) *N*-alkylpyridylporphyrins of different alkyl chain length [52]. The yeast study offers additional insight into why otherwise excessively hydrophilic MnTE-2-PyP^{5+} and to a much higher extent lipophilic MnTnHex-2-PyP^{5+} accumulate in the mitochondria: the cytosolic-based reduction, accompanied by a remarkable gain in lipophilicity, may be at least in part a driving force for their mitochondrial accumulation.

Accumulation of MnPs in tumours—Along with MRI imaging data [53], this set of data clearly show preferred accumulation of MnPs in tumour than in a normal tissue.

Higher tumour accumulation of cationic MnPs may be due to several reasons. In general, and as already stated, the tumour leaky vasculature facilitates higher accumulation of any administered drug [47]. Further, cancer cells have a higher surface area than the normal cell, because of the higher number of microvilli and more chances to interact with a drug [54,55]. Finally, in contrast to the normal cell, which expresses mostly neutral zwitterionic phospholipids and sterols on its surface [56], cancer cells have a net negative surface charge, due to the higher expression of anionic molecules, such as phosphatidylserine, *O*-glycosylated mucins, sialilated gangliosides and heparin sulphates [57]. These negatively charged molecules facilitate interaction and penetration of the cationic species through the

membrane [55–59]. It has been shown that some cationic porphyrins bind to anionic regions of proteins, such as human serum albumin, which transports them into the tumour [60–62]. Porphyrins studied were *para* isomers, MnTM-4-PyP^{5+} and Mn(III) *meso*-tetrakis (4-*N*, *N*, *N*-trimethylanilinium) porphyrin. Datta-Gupta et al. [61] showed that metal-free analogues of *N*-alkylpyridylporphyrins we studied herein (the isomeric metal-free *N*-methylpyridylporphyrins *ortho*, *meta* and *para* H_2TM-(2 or 3 or 4)-PyP^{4+}) bind on the surface of albumin, at a site near to tryptophan residue, rather than sliding in a crevise of human serum albumin.

Mechanism of action—Most cells have abundant levels of ascorbate. In the presence of ascorbate, redox-able MnPs may act as pro-oxidants and catalyse oxygen consumption of ascorbate resulting in the production of $O_2^{\cdot -}/H_2O_2$ [22], which in turn may cause cancer cell death [16,19,21]. Under physiological conditions with an abundance of peroxide-removal systems, such redox cycling of ascorbate (which should have otherwise been catalysed by endogenous Fe porphyrins [19]) may not be damaging. In general, integrity of tumour is compromised; it is under constant oxidative stress and deficient in endogenous antioxidant defenses relative to normal cells [4]. Tumour employs such deficiency to its advantage to support its aggressive proliferation [4]. We have already shown that MnTE-2-PyP^{5+} closely mimics MnSOD in skin carcinogenesis; the anti-oxidative action was suggested [51]. The same action was proposed for the role of MnTE-2-PyP^{5+} in a mouse 4T1 breast cancer study [38]. While MnP itself is not toxic to tumour cells [16], the data suggest that it suppresses tumour growth via anti-angiogenic mode of action [38]. Such anti-oxidative action was explained to result fom the removal of signaling reactive species and suppression of HIF-1α activation and VEGF expression, which in turn results in suppression of tumour vasculature growth [38]. When coupling with endogenous or exogenous ascorbate, MnP could increase cellular oxidative burden and eventually suppress tumour growth via pro-oxidative action in a way already suggested and fairly justified for the enzyme MnSOD itself [11,63–68]. Kim et al. [17] provided convincing evidence that overexpression of MnSOD in liver cells (or by the analogy the administration of MnTE-2-PyP^{5+}) increases oxidative burden. Yet, the cells seemingly counterfight with adaptive response, i.e. subsequent upregulation of endogenous antioxidant defenses. In turn, the signs of suppressed oxidative stress may be observed and ascribed to the anti-oxidative action of MnSOD. By analogy, the mimic of MnSOD may be operating in similar ways. Future work on mechanistic aspects of SOD mimics is in progress.

The most obvious case of the pro-oxidative action of MnP, under biologically relevant reducing conditions, was observed in a very simple and straightforward system, the aerobic growth of SOD-deficient *E. coli*. The *E. coli* growth assay is superoxide-specific [1]. It has been shown in numerous studies that the SOD-deficient *E. coli*, which lacks cytosolic SODs, grows very poorly aerobically. However, it grows as well as wild type when the medium is supplied with efficacious SOD mimic. Yet, if the medium contains both MnTE-2-PyP^{5+} and ascorbate, the growth of SOD-deficient *E. coli* was fully suppressed; the same has been observed with wild type. Another obvious case is the growth of different cancer cells in the presence of MnP/ascorbate [16]. Neither MnP nor ascorbate were toxic under concentrations where the combined treatment killed four different cancer cells ([16], Fels et al. unpublished). The pro-oxidative mode of action was also seen in our *in vivo* 4T1 breast cancer mouse study when MnTnHex-2-PyP^{5+} was co-administerd with ascorbate ([16], Fels et al. unpublished); our data are in agreement with the Levine et al. [19] study where ascorbate administration killed different tumours via peroxide formation catalyzed by endogenous antioxidants. The combined use of MnP/ascorbate may have dual benefit in cancer therapy: (1) the gain in lipophilicity upon reduction would facilitate MnP transport into the cell and critical sub-cellular compartments (mitochondria, nucleus etc), whereas (2)

MnP-driven catalysis of oxygen reduction by ascorbate would enhance tumour growth suppression via excessive pro-oxidative damage.

The mere fact that MnP can easily attain four oxidation states *in vivo* (+2, +3, +4 and +5), each of them with its own protonation/deprotonation equilibria (detailed in [69] and [70]), suggests a complex biology of Mn porphyrins. Further studies are needed to comprehend the role of endogenous and exogenous antioxidants in cancer therapy.

Ortho vs meta MnTE-2-PyP^{5+}

When given ip at 10 mg/kg to mouse, within 30 min MnTE-2-PyP^{5+} reaches ~20 μM plasma levels (6-fold less than injected) [39]; i.e. similar to the levels of ascorbate. Under the same conditions, *meta* Mn^{III}TE-3-PyP^{5+} would cross the plasma membrane more readily than *ortho*, as it is more lipophilic (Table II) [25]. In the cell, where *ortho* and *meta* are equally reducible, their lipophilicity would have increased 100- and 10-fold, respectively, and they would have had the same probability to reach mitochondria. However, Ferrer-Sueta et al. [27] showed that MnTM-4-PyP^{5+} analogue of similar reducibility as MnTE-3-PyP^{5+} (Table I) [1,2,12,27] can not be as readily reduced *in vivo* as *ortho* MnTE-2-PyP^{5+}. Further, antioxidant capacity, conveniently expressed as k_{cat} ($O_2^{\cdot -}$), is 10-fold lower for *meta* than for *ortho*. Based on this evidence, once both isomers cross the plasma membrane, *ortho* analogue may have a higher chance to reach mitochondria and scavenge ROS/RNS. Unless lipophilicity of *meta* Mn^{III}TE-3-PyP^{5+} is a critical factor that controls the extent to which the MnP crosses plasma membrane and reaches cell interior and therefore presides over its destiny within the cell.

Conclusions

Endogenous reductants + MnP

Within the cell, the *ortho* Mn porphyrins get easily reduced with cellular reductants. Such reduction is likely coupled to a catalytic scavenging of reactive oxygen and nitrogen species. Upon reduction, they lose a single charge from Mn site, whereby they become up to three orders more lipophilic. Such gain in lipophilicity facilitates their cellular and sub-cellular accumulation. The increase in lipophilicity upon reduction was observed with both *ortho* and *meta* isomers. Its magnitude is related to the length of alkyl chain and the type of isomer in a bell shape fashion as a consequence of the interplay between the solvation, steric and lipophilicity effects. All effects are more pronounced with *ortho* than with *meta* isomers.

Exogenous reductants + MnP

The ascorbate levels in plasma and extracellular fluids are significantly lower than within the cell and may not be enough to stabilize MnPs in the reduced state. Thus, their administration with ascorbate would facilitate their reduction in plasma, whereby lipophlicity and, in turn, transport across the plasma membrane gets enhanced.

Relevance to anti-cancer therapy

Our data further show that MnP accumulates 5-fold more in tumour than in surrounding muscle, which was enhanced with exogenously added ascorbate and strengthens their development as anti-cancer drugs and tumour imaging agents. Future studies will address (1) if MnPs anti-cancer efficacy could be enhanced when they are co-administered with reductants; (2) whether co-administration with ascorbate affects the MnP mechanism of action and if this is dependent upon the cancer cell oxidative burden (relative to normal cell) and (3) which are better drug candidates: *ortho* or *meta* isomers.

Acknowledgments

IBH, ZR, IK, KL, XY and MWD acknowledge the financial help from Wallace H. Coulter Translational Partners Grant Program and from the National Institutes for Allergy and Infectious Diseases (U19AI0 677989). IBH is also grateful to R01 DA 024074. IS thanks NIH/NCI Duke Comprehensive Cancer Center Core Grant (5-P30-CA14236-29). DF, CD and MWD are thankful to CA40355-25, LB to Kuwait University, grant MB03/07, ZV to R01 CA098452 and U19AI0677989, and JSR to Universidade Federal da Paraíba. XDY is very grateful to the financial support from Hefei National Laboratory for Physical Sciences at the Microscale at University of Science and Technology of China during his stay in Professor Kam W. Leong group at Duke University.

Abbreviations

Asc	sodium ascorbate
$CO_3^{\bullet-}$	carbonate radical
$E_{1/2}$	half-wave reduction potential
HFBA	heptafluorobutyric acid
H_2O_2	hydrogen peroxide
HClO	hypochlorous acid
ip	intraperitoneal
k_{cat}	rate constant for $O_2^{\bullet-}$ dismutation
meso	5,10,15,20 positions on porphyrin ring
MnP	Mn porphyrin
Herein	oxidized MnP relates to complexes ($Mn^{III}P$) where Mn is in + 3 oxidation state, relative to complexes ($Mn^{II}P$) where Mn is in +2 oxidation state
MnTalkyl-2(or 3 or 4)-PyP^{5+}	Mn(III) meso-tetrakis(N-alkylyridinium-2(or 3 or 4)-yl)porphyrin, alkyl being methyl (M), ethyl (E), n-propyl (nPr, also Pr), n-butyl (nBu, also Bu), n-hexyl (nHex, also Hex), n-heptyl (nHep, also Hep), n-octyl (nOct, also Oct)
2, 3 and 4 relate to ortho	meta and para isomers, respectively
MnTM-2-PyP^{+} (AEOL10112)	MnTE-2-PyP^{5+} (AEOL10113, FBC-007), MnTDE-2-ImP^{5+}, Mn(III) meso-tetrakis(N,N'-diethylimidazolium-2-yl)porphyrin, AEOL10150
H_2TM-2(or 3 or 4)-PyP^{5+}	meso-tetrakis(N-methylpyridinium-2(or 3 or 4)-yl)porphyrin
MS	mass spectroscopy
LC/ESI-MS/MS	liquid chromatography/electrospray ionization-tandem mass spectrometry
MRI	magnetic resonance imaging
NHE	normal hydrogen electrode
$^{\bullet}$NO	nitric oxide
$O_2^{\bullet-}$	superoxide

$ONOO^-$	peroxynitrite, $ONOO^-$ + ONOOH, given its pK_a = 6.6 at pH 7.8 peroxynitrite exists predominantly as $ONOO^-$
P_{OW}	partition coefficient between n-octanol and water
R_f	thin-layer chromatographic retention factor
sc	subcutaneous
SOD	superoxide dismutase
TLC	thin-layer chromatography
ZnP	Zn porphyrin
ZnTE-2-PyP^{4+}	Zn(II) meso-tetrakis(N-ethylpyridinium-2-yl)porphyrin
bFGF	basic fibroblast growth factor
DUOX	dual oxidase
NOX	NADPH oxidase
PDGF	platelet-derived growth factor
VEGF	vascular endothelial growth factor

References

1. Batinić-Haberle I, Rebouças JS, Spasojević I. Superoxide dismitase mimics: chemistry, pharmacology, and therapeutic potential. Antioxid Redox Signal. 2010; 13:877–918. [PubMed: 20095865]
2. Batinić-Haberle, I.; Reboucas, JS.; Benov, L.; Spasojevic, I. Chemistry, biology and medical effects of water soluble metalloporphyrins. In: Kadish, KM.; Smith, KM.; Guillard, R., editors. Handbook of porphyrin science. Vol. Vol11. World Scientific; 2010.
3. Kietzmann T. Intracellular redox compartments: mechanisms and significances. Antioxid Redox Signal. 2010; 13:395–398. [PubMed: 20136596]
4. Halliwell, B.; Gutteridge, JMC. Free radicals in biology and medicine. 4th ed.. New York: Oxford University Press; 2007. p. 79-186.
5. Takeya R, Sumimoto H. Regulation of novel superoxide-producing NADP(H) oxidases. Antioxid Redox Signal. 2006; 8:1523–1532. [PubMed: 16987008]
6. Leto TL, Morand S, Hurt D, Ueyama T. Targeting and regulation of reactive oxygen species generation by Nox family NADPH oxidases. Antioxid Redox Signal. 2009; 11:2607–2619. [PubMed: 19438290]
7. Petry A, Weitnauer M, Görlach A. Receptor activation of NADPH oxidases. Antioxid Redox Signal. 2010; 13:467–487. [PubMed: 20001746]
8. Weinberg F, Chandel NS. Reactive oxygen species-dependent signaling regulates cancer. Cell Mol Life Sci. 2009; 66:3663–3673. [PubMed: 19629388]
9. Cerutti PA. Pro-oxidant states and tumor promotion. Science. 1985; 227:375–381. [PubMed: 2981433]
10. Storz P. Reactive oxygen species in tumor progression. Front Biosci. 2005; 10:1881–1896. [PubMed: 15769673]
11. Holley AK, Dhar SK, Xu Y, St. Clair DK. Manganese superoxide dismutase: beyond life and death. Amino Acids. 2010
12. Batinić-Haberle I, Spasojević I, Tse HM, Tovmasyan A, Rajic Z, St. Clair DK, Vujasković Z, Dewhirst MW, Piganelli JD. Design of Mn porhyrins for treating oxidative stress injuries and their redox-based regulation of celluler transcriptional activities. Amino Acids. 2010

13. Spasojević I, Yumin C, Noel T, Yu I, Pole MP, Zhang L, Zhao Y, St Clair DK, Batinić-Haberle I. Mn porphyrin-based SOD mimic, MnTE-2-PyP^{5+} targets mouse heart mitochondria. Free Radic Biol Med. 2007; 42:1193–1200. [PubMed: 17382200]
14. Ferrer-Sueta G, Vitturi D, Batinić-Haberle I, Fridovich I, Goldstein S, Czapski G, Radi R. Reactions of manganese porphyrins with peroxynitrite and carbonate radical anion. J Biol Chem. 2003; 278:27432–27438. [PubMed: 12700236]
15. Jaramillo MC, Frye JB, Crapo JD, Briehl MM, Tome ME. Increased manganese superoxide dismutase expression or treatment with manganese porphyrin potentiates dexamethasone-induced apoptosis in lymphoma cells. Cancer Res. 2009; 69:5450–5457. [PubMed: 19549914]
16. Ye X, Fels D, Dedeugd C, Dewhirst MW, Leong K, Batinić-Haberle I. The *in vitro* cytotoxic effects of Mn(III) alkylpyridylporphyrin/ascorbate system on four tumor cell lines. Free Radic Biol Med. 2009; 47:136.
17. Kim A, Joseph S, Khan A, Epstein CJ, Sobel R, Huang T-T. Enhanced expression of mitochondrial superoxide dismutase leads to prolonged *in vivo* cell cycle progression and up-regulation of mitochondrial thioredoxin. Free Radic Biol Med. 2010; 48:1501–1512. [PubMed: 20188820]
18. Spasojević I, Batinić-Haberle I, Fridovich I. Nitrosylation of manganese(II) tetrakis(*N*-ethylpyridinium-2-yl)porphyrin. Nitric Oxide. 2000; 4:526–533. [PubMed: 11020341]
19. Levine M, Conry-Cantilena C, Wang Y, Welch RW, Washko PW, Dhariwal KR, Park JB, Lazarev A, Graumlich JF, King J, Cantilena LR. Vitamin C pharmacokinetics in healthy volunteers: evidence for a recommended dietary allowance. Proc Natl Acad Sci USA. 1996; 93:3703–3709.
20. Spasojevic I, Colvin OM, Warshany KR, Batinic-Haberle I. New approach to the activation of anti-cancer pro-drugs by metalloporphyrin-based cytochrome P450 mimics in all-aqueous biologically relevant system. J Inorg Biochem. 2006; 100:1897–1902. [PubMed: 16965820]
21. Rajic Z, Benov L, Kos I, Tovmasyan A, Batinic-Haberle I. Cationic Mn porphyrins change their action from anti- to pro-oxidative in the presence of cellular reductants. Relevance to understanding beneficial therapeutic effects of SOD mimics *in vivo*. Free Radic Biol Med. 2010; 49S Book of Abstracts.
22. Batinić-Haberle I, Spasojević I, Stevens RD, Ham-bright P, Fridovich I. Manganese(III) *meso* tetrakis *ortho N*-alkylpyridylporphyrins: synthesis, characterization and catalysis of $O_2^{\cdot -}$dismutation. J Chem Soc Dalton Trans. 2002:2689–2696.
23. Okado-Matsumoto A, Batinić-Haberle I, Fridovich I. Complementation of SOD deficient *Escherichia coli* by manganese porphyrin mimics of superoxide dismutase. Free Radic Biol Med. 2004; 37:401–410. [PubMed: 15223074]
24. Pollard JM, Rebouças JS, Durazo A, Kos I, Fike F, Panni M, Gralla EB, Valentine JS, Batinić-Haberle I, Gatti RA. Radio-protective effects of manganese-containing superoxide dismutase mimics on ataxia telangiectasia cells. Free Radic Biol Med. 2009; 47:250–260. [PubMed: 19389472]
25. Kos I, Benov L, Spasojević I, Rebouças JS, Batinić-Haberle I. High lipophilicity of *meta* Mn(III) *N*-alkylpyridylporphyrin-based SOD mimics compensates for their lower antioxidant potency and makes them equally effective as *ortho* analogues in protecting SOD-deficient *E. coli.* J. Med Chem. 2009; 52:7868–7872. [PubMed: 19954250]
26. Kos I, Rebouças JS, DeFreitas-Silva G, Salvemini D, Vujasković Z, Dewhirst MW, Spasojević I, Batinić-Haberle I. Lipophilicity of potent porphyrin-based antioxidants: comparison of *ortho* and *meta* isomers of Mn(III) *N*-alkylpyridylporphyrins. Free Radic Biol Med. 2009; 47:72–78. [PubMed: 19361553]
27. Ferrer-Sueta G, Hannibal L, Batinić-Haberle I, Radi R. Reduction of manganese porphyrins by flavoenzymes and submitochondrial particles and the catalytic redox cycle of peroxynitrite. Free Radic Biol Med. 2006; 41:503–512. [PubMed: 16843831]
28. Kachadourian R, Johnson CA, Min E, Spasojevic I, Day BJ. Flavin-dependent antioxidant properties of a new series of *meso-N,N'*-dialkyl-imidazolium substituted manganese(III) porphyrins. Biochem Pharmacol. 2004; 67:77–85. [PubMed: 14667930]
29. Batinić-Haberle I, Spasojević I, Fridovich I. Tetrahydrobiopterin rapidly reduces the SOD mimic Mn(III) *ortho*-tetrakis (*N*-ethylpyridinium-2-yl)porphyrin. Free Radic Biol Med. 2004; 37:367–374. [PubMed: 15223070]

30. Ferrer-Sueta G, Batinić-Haberle I, Spasojević I, Fridovich I, Radi R. Catalytic scavenging of peroxynitrite by isomeric Mn(III) *N*-methylpyridylporphyrins in the presence of reductants. Chem Res Toxicol. 1999; 12:442–449. [PubMed: 10328755]

31. Batinić-Haberle I, Benov L, Spasojević I, Fridovich I. The *ortho* effect makes manganese (III) *meso*-tetrakis(*N*-methylpyridinium-2-yl)porphyrin (MnTM-2-PyP) a powerful and potentially useful superoxide dismutase mimic. J Biol Chem. 1998; 273:24521–24528. [PubMed: 9733746]

32. Batinić-Haberle I, Benov L, Spasojević I, Hambright P, Crumbliss AL, Fridovich I. The relationship between redox potentials, proton dissociation constants of pyrrolic nitrogens, and *in vitro* and *in vivo* superoxide dismutase activities of manganese(III) and iron(III) cationic and anionic porphyrins. Inorg Chem. 1999; 38:4011–4022.

33. Rebouças JS, Kos I, Vujasković Z, Batinić-Haberle I. Determination of residual manganese in Mn porphyrin-based superoxide dismutase (SOD) and peroxynitrite reductase mimics. J Pharm Biomed Anal. 2009; 50:1088–1091. [PubMed: 19660888]

34. Imlay JA, Linn S. Mutagenesis and stress responses induced in *Escherichia coli* by hydrogen peroxide. J Bacteriol. 1987; 169:2967–2976. [PubMed: 3298208]

35. B atinić-Haberle I, Cuzzocrea S, Rebouças JS, Ferrer-Sueta G, Mazzon E, Di Paola R, Radi R, Spasojević I, Benov L, Salvemini D. Pure MnTBAP selectively scavenges peroxynitrite over superoxide: comparison of pure and commercial MnTBAP samples to MnTE-2-PyP in two different models of oxidative stress injuries, SOD-specific *E. coli* model and carrageenan-induced pleurisy. Free Radic Biol Med. 2009; 46:192–201. [PubMed: 19007878]

36. Lowry OH, Rosebrough NJ, Farr AL, Randall RJ. Protein measurement with the folin phenol reagent. J Biol Chem. 1951; 193:265–275. [PubMed: 14907713]

37. Chen Q, Espey MG, Sun AY, Pooput C, Kirk KL, Krishna MC, Khosh DB, Drisko J, Levine M. Pharmacologic doses of ascorbate act as pro-oxidant and desrease growth of aggressive tumor xenografts in mice. Proc Natl Acad Sci USA. 2008; 105:11105–11109. [PubMed: 18678913]

38. Rabbani ZN, Spasojević I, Zhang X, Moeller BJ, Haberle S, Vasquez-Vivar J, Dewhirst MW, Vujasković Z, Batinić-Haberle I. Antiangiogenic action of redox-modulating Mn(III) *meso*-tetrakis(*N*-ethylpyridinium-2-yl)porphyrin, MnTE-2-PyP^{5+}, *via* suppression of oxidative stress in a mouse model of breast tumor. Free Radic Biol Med. 2009; 47:992–1004. [PubMed: 19591920]

39. Spasojević I, Chen Y, Noel TJ, Fan P, Zhang L, Rebouças JS, St Clair DK, Batinić-Haberle I. Pharmacokinetics of the potent redox modulating manganese porphyrin, MnTE-2-PyP^{5+} in plasma and major organs of B6C3F1 mice. Free Radic Biol Med. 2008; 45:943–949. [PubMed: 18598757]

40. Miele M, Fillenz M. *In vivo* determination of extracellular brain ascorbate. J Neurosci Methods. 1996; 70:15–19. [PubMed: 8982976]

41. Schenk JO, Miller E, Gaddis R, Adams RN. Homeostatic control of ascorbate concentration in CNS extracellular fluid. Brain Res. 1982; 253:353–356. [PubMed: 6295558]

42. Mandl J, Szarka A, Banhegyi G. Vitamin C: update on physiology and pharmacology. Brit J Pharmacol. 2009; 157:1097–1110. [PubMed: 19508394]

43. Eric D, Culter ED, Emerson JP, Kurtz DM Jr, Cabelli DE. Superoxide reactivity of rubredoxin oxidoreductase (desulfoferrodoxin) from *Desulfovibrio vulgaris*: a pulse radiolysis study. J Am Chem Soc. 2000; 122:11555–11556.

44. Ferrer-Sueta G, Quijano C, Alvarez B, Radi R. Reactions of manganese porphyrins and manganese-superoxide dismutase with peroxynitrite. Methods Enzymol. 2002; 349:23–37. [PubMed: 11912912]

45. Engelmann FM, Rocha SVO, Toma HE, Araki K, Baptista MS. Datermination od n-octanol/water partition and membrane binding of cationic porphyrins. Int J Pharm. 2007; 329:12–18. [PubMed: 16979860]

46. Batinic-Haberle I, Stevens R, Fridovich I. Electrospray mass spectrometry of isomeric tetrakis-(*N*-alkylpyridyl)porphyrins and their manganese(III) and iron(III) complexes. J Porphyrins Phthalocyanines. 2000; 4:217–227.

47. Torchilin VP. Passive and active drug targeting: drug delivery to tumors as an example. Handb Exp Pharmacol. 2010; 197:3–53. [PubMed: 20217525]

48. Riches AC, Sharp JG, Brynmor Thomas D, Vaughan Smith S. Blood volume determination in the mouse. J Physiol. 1973; 228:279–284. [PubMed: 4687099]

49. Tsao CS, Leung PY, Young M. Effect of dietary ascorbic acid intake on tissue vitamin C in mice. J Nutrition. 1987; 117 291-197.
50. Murphy MP. Targeting lipophilic cations to mitochondria. Biochim Biophys Acta. 2008; 177:1028–1031. [PubMed: 18439417]
51. Zhao Y, Chaiswing L, Oberley TD, Batinić-Haberle I, St Clair W, Epstein CJ, St Clair DK. A mechanism-based antioxidant approach for the reduction of skin carcinogenesis. Cancer Res. 2005; 65:1401–1405. [PubMed: 15735027]
52. Spasojevic I, Li AM, Tovmasyan A, Rajic Z, Salvemini D, St. Clair D, Valentine JS, Vujaskovic Z, Gralla EB, Batinic-Haberle I. Accumulation of porphyrin-based SOD mimics in mitochondria is proportional to their lipophilicity. *S. cerevisiae* study of *ortho* Mn(III) *N*-alkylpyridylporphyrins. Free Radic Biol Med. 2010; 49S Book of abstracts.
53. Lascola, CD.; Batinić-Haberle, I.; Venkatraman, T.; Amrheim, T.; Mouraviev, V.; Wang, H. Mn-porphyrins SOD mimetics as novel NMR imaging probes. 6th International Conference on Porphyrins and Phthalocyanines, ICPP-6; New Mexico. 2010.
54. Chan SC, Hui L, Chen HM. Enhancement of the cytolytic effect of anti-bacterial peptide cecropin by the microvilli of cancer cells. Anticancer Res. 1998; 18:4467–4474. [PubMed: 9891511]
55. Zwaal RF, Schroit AJ. Pathophysiologic implications of membrane phospholipid asymmetry in blood cells. Blood. 1997; 89:1121–1132. [PubMed: 9028933]
56. Hoskin DW, Ramamoorthy A. Studies on anticancer activities of antimicrobial peptides. Biochim Biophys Acta. 2008; 1778:357–375. [PubMed: 18078805]
57. Schweizer F. Cationic amphiphilic peptides with cancer-selective toxicity. Eur J Pharmacol. 2009; 625:190–194. [PubMed: 19835863]
58. Kornguth SE, Kalianke T, Robins HI, Cohen JD, Turski P. Preferential binding of radiolabeled poly-L-lysine to C6 and U87 MG glioblastomas compared to endothelial cells *in vitro*. Cancer Res. 1989; 49:6390–6395. [PubMed: 2804985]
59. Jensen TJ, Vicente MGH, Luguya R, Norton J, Fronczek FR, Smith KM. Effect of overall charge and charge distribution on cellular uptake, distribution and phototoxicity of cationic porphyrins in Hep2 cells. J Photochem Photobiol B: Biol. 2010; 100:100–111.
60. Zhou B, Zhang Z, Zhang Y, Li R, Xiao Q, Liu Y, Li Z. Binding of cationic porphyrin to human serum albumin studied using comprehensive spectroscopic methods. J Pharm Sci. 2009; 98:105–113. [PubMed: 18464274]
61. Datta-Gupta N, Malakar D, Walters E, Thompson B. Binding studies of three water-soluble polycationic porphyrins with human serum albumin. Res Commun Chem Pathol Pharmacol. 1988; 60:347–360. [PubMed: 3175333]
62. Ma H-M, Chen X, Zhang N, Han Y-Y, Wu D, Du B, Wei Q. Spectroscopic studies on the interaction of a water-soluble cationic porphyrin with proteins. Spectrochim Acta, Part A: Mol Biomol Spectroscopy. 2009; 72:465–469.
63. Li S, Yan T, Yang J-Q, Oberley TD, Oberley LW. The role of cellular glutathione peroxidase redox regulation in the suppression of tumor cell growth by manganese superoxide dismutase. Cancer Res. 2000; 60:3927–3939. [PubMed: 10919671]
64. Buettner GR, Ng CF, Wang M, Rodgers VG, Schafer FQ. A new paradigm: manganese superoxide dismutase influences the production of H_2O_2 in cells and therby their biological state. Free Radic Biol Med. 2006; 41:1338–1350. [PubMed: 17015180]
65. Rodriguez AM, Carrico PM, Mazurkiewicz JE, Melendez JA. Mitohondrial or cytosolic catalase reverses the MnSOD-dependent inhibition of proliferation by enhancing respiratory chain activity, net ATP production, and decreasing the steady state levels of H_2O_2. Free Radic Biol Med. 2000; 29:801–813. [PubMed: 11063906]
66. Darby Weydert CJ, Smith BB, Xu L, Kregel KC, Ritchie JM, Davis CS, Oberley LW. Inhibition of oral cancer cell growth by adenovirus MnSOD plus BCNU treatment. Free Radic Biol Med. 2003; 34:316–329. [PubMed: 12543247]
67. Ridnour LA, Oberley TD, Oberley LW. Tumor supressive effects of MnSOD overexpression may involve imbalance in peroxide generation versus peroxide removal. Antiox Redox Signal. 2004; 6:501–512.

68. Amstad P, Moret R, Cerutti P. Glutathione peroidase compensates for the hypersensitivity of Cu,Zn-superoxide overproducers to oxidant stress. J Biol Chem. 1994; 269:1606–1609. [PubMed: 8294405]

69. Budimir A, Smuc T, Weitner T, Batinic-Haberle I, Birus M. Thermodynamics and electrochemistry of manganese tetra (*ortho-n*-butylpyridyl)porphyrin in aqueous solutions. J Coord Chem. 2010; 63:2750–2765.

70. Weitner T, Budimir A, Kos I, Batinić-Haberle I, Biruš M. Acid-base and electrochemical properties of manganese *meso(ortho-* and *meta*-ethylpyridyl)porphyrins: potentiometric, spectrophotometric and spectroelectrochemical study of protolytic and redox equilibria. Dalton Trans. 2010 in press.

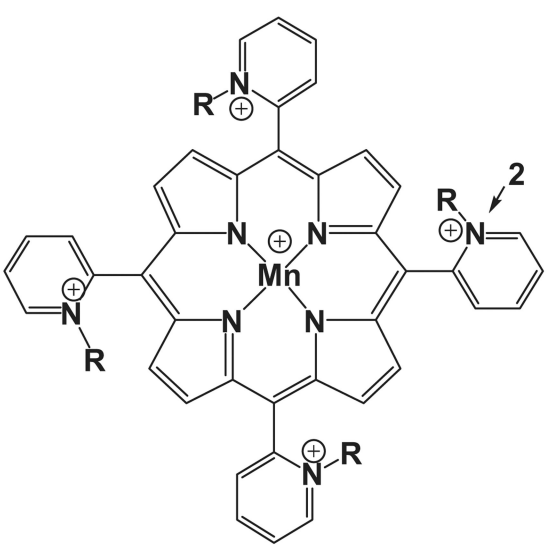

***Ortho* isomers**

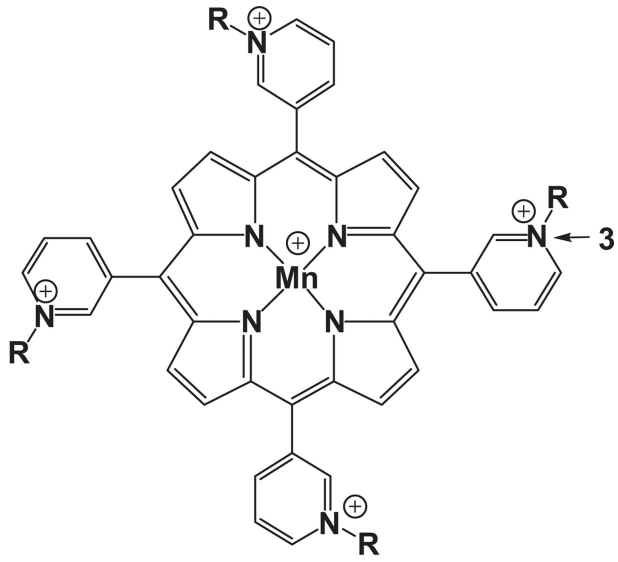

***Meta* isomers**

MnTM-2-PyP^{5+} = M-2:	R=**M**ethyl
MnTE-2-PyP^{5+} = E-2:	R=**E**thyl
MnTnPr-2-PyP^{5+} = nPr-2:	R=**n-Pr**opyl
MnTnBu-2-PyP^{5+}= nBu-2:	R=**n-Bu**tyl
MnTnHex-2-PyP^{5+} = nHex-2:	R=**n-Hex**yl
MnTnHep-2-PyP^{5+} = nHep-2:	R=**n-Hep**tyl
MnTnOct-2-PyP^{5+} = nOct-2:	R=**n-Oct**yl

MnTM-3-PyP^{5+} = M-3:	R=**M**ethyl
MnTE-3-PyP^{5+} = E-3:	R=**E**thyl
MnTnPr-3-PyP^{5+} = nPr-3:	R=**n-Pr**opyl
MnTnBu-3-PyP^{5+}= nBu-3:	R=**n-Bu**tyl
MnTnHex-3-PyP^{5+} = nHex-3:	R=**n-Hex**yl

Figure 1.
Structures of *ortho* and *meta* Mn(III) *N*-alkylpyridylporphyrins.

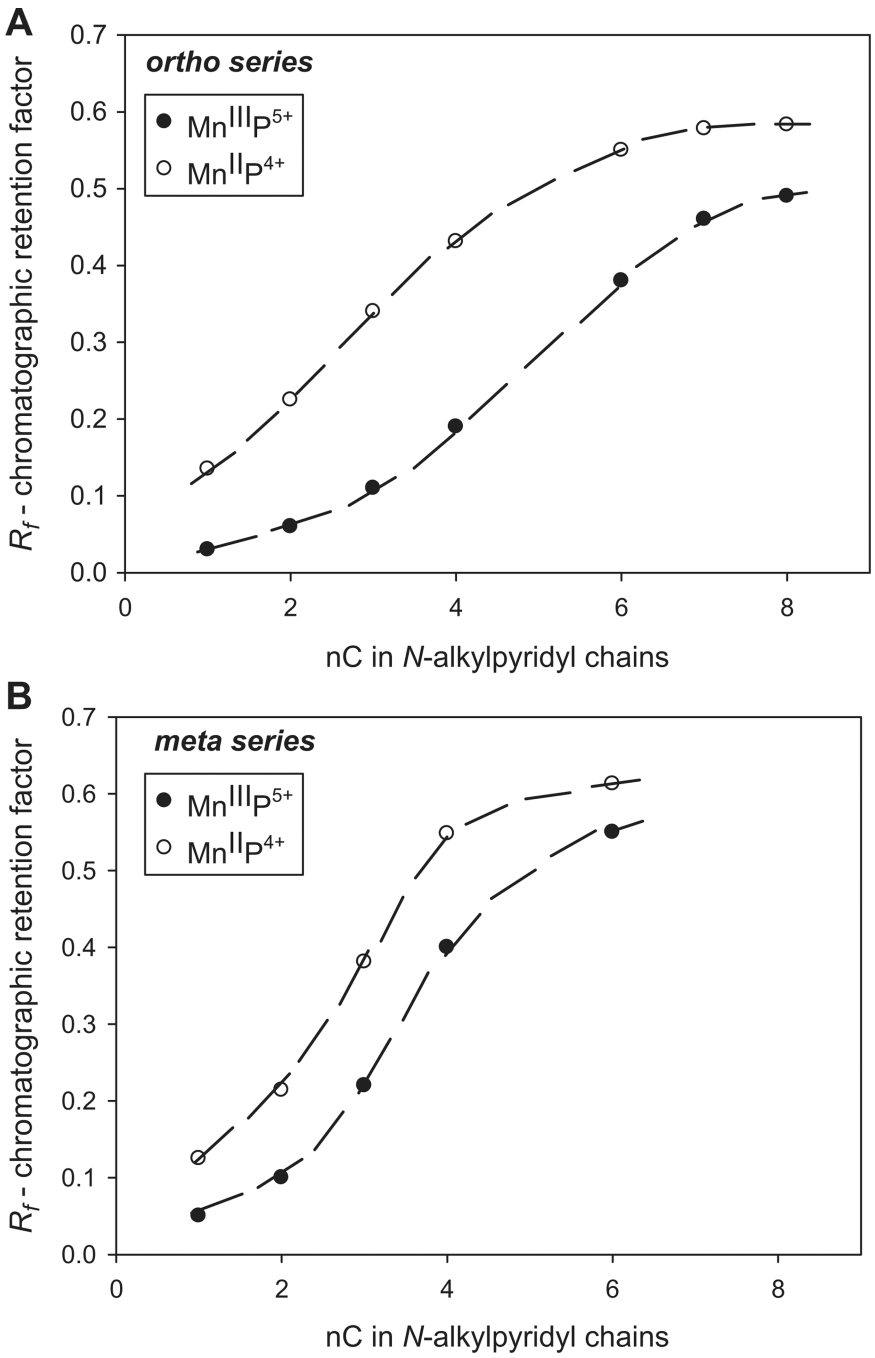

Figure 2.

Relationship between the chromatographic retention factor (R_f) and the number of carbon atoms (nC) in alkyl chains for the series of *ortho* (A) and *meta* (B) oxidized ($Mn^{III}P^{5+}$) and reduced ($Mn^{II}P^{4+}$) Mn *N*-alkylpyridylporphyrins. Filled circles represent Mn^{III}Ps, while empty circles represent Mn^{II}Ps, respectively.

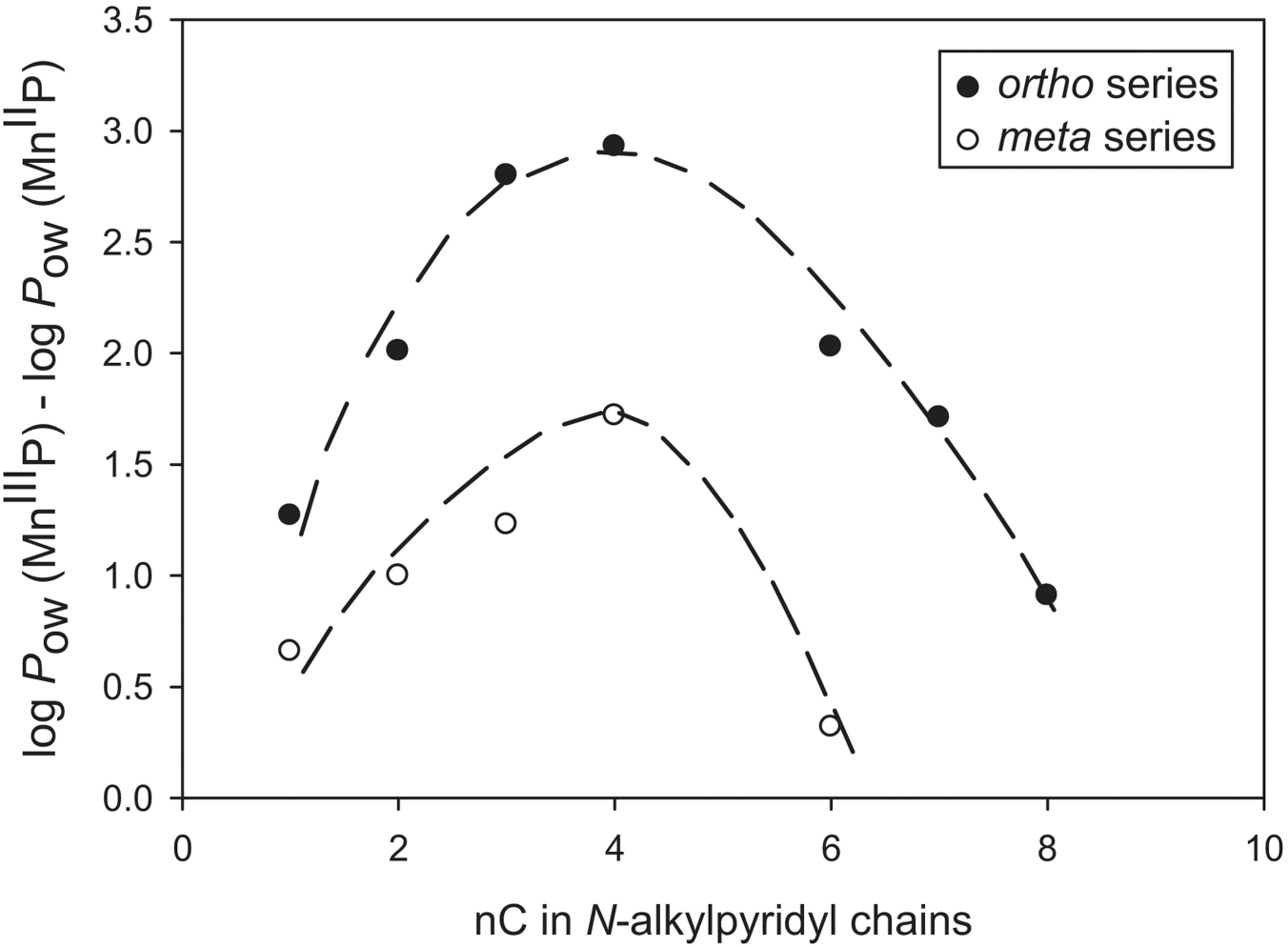

Figure 3.
The effect of $Mn^{III}P^{5+}$ to $Mn^{II}P^{4+}$ reduction on lipophilicity (described as log P_{OW}) as influenced by the length of *N*-alkylpyridyl chains (described as the number of carbon atoms in the chains, nC).

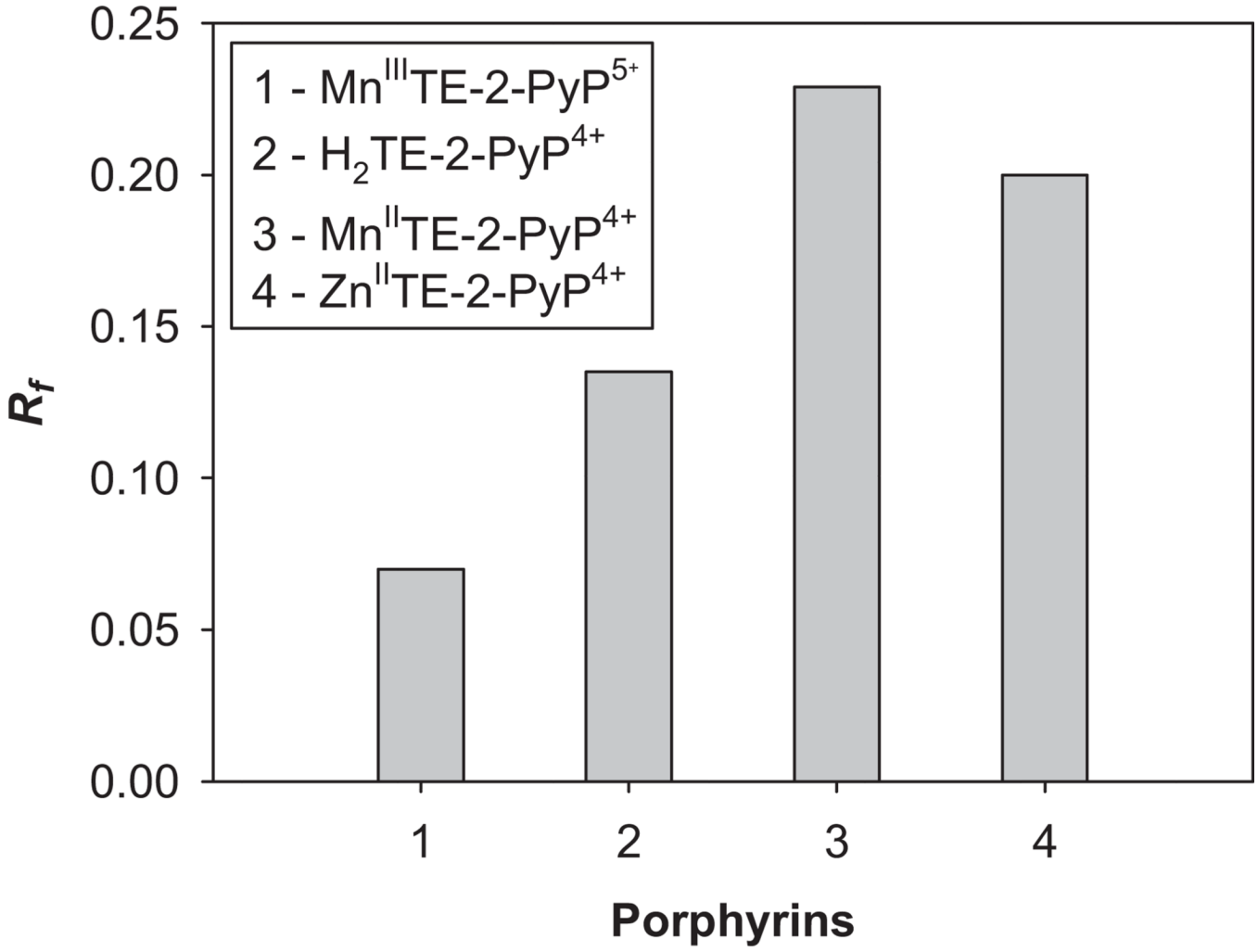

Figure 4.
The effect of the type of porphyrin bearing the same tetracationic charge on its lipophilicity. All tetracationic compounds are more lipophilic than pentacationic $Mn^{III}TE-2-PyP^{5+}$. The most lipophilic was reduced $Mn^{II}TE-2-PyP^{4+}$.

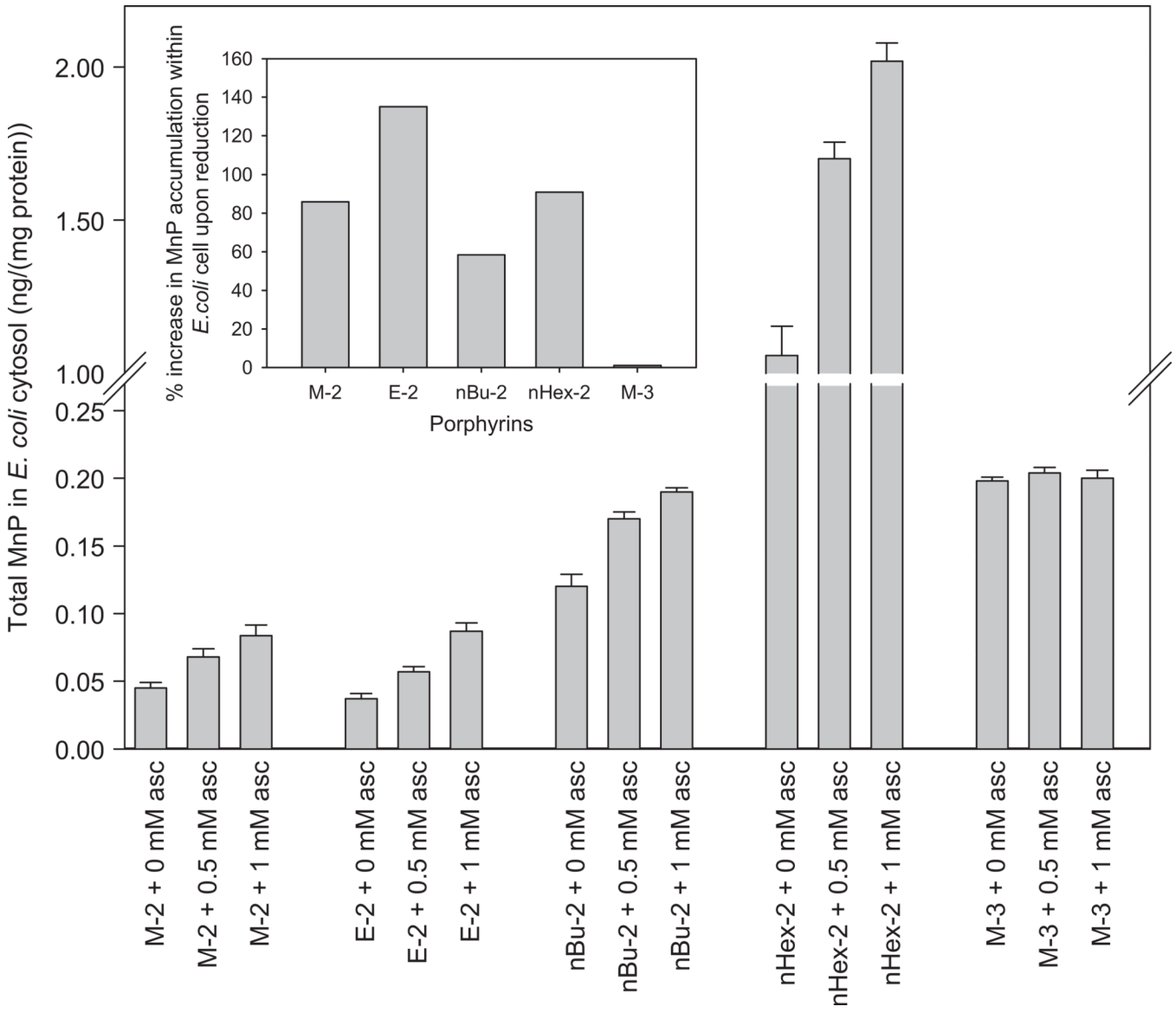

Figure 5.

Cytosolic accumulation of Mn *N*-alkylpyridylporphyrins. *E. coli* (AB1157) grew in casamino M9CA medium for 1 h in the presence of 5 μM MnPs and in the presence or absence of 0.5 and 1 mM sodium ascorbate. Inset: The effect of the reduction of MnP on *E. coli* cytosolic accumulation. The effect depends upon MnP/ascorbate ratio.

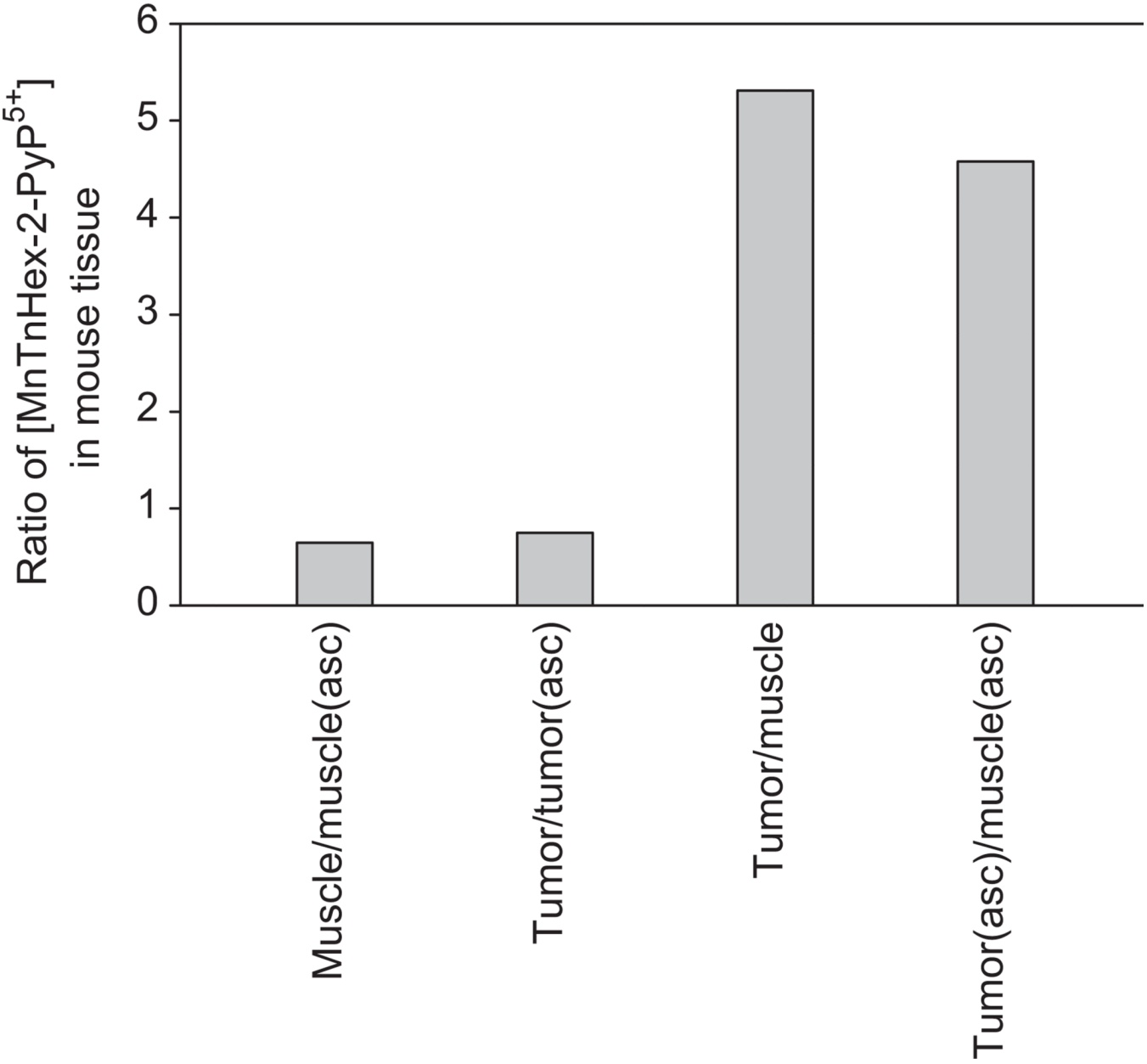

Figure 6.
The ratios of the levels of MnTnHex-2-PyP^{5+} in muscle and tumour when administered with and without ascorbate. The first two bars indicate the enhancement in MnP accumulation as influenced by ascorbate. The last two bars show the preferred accumulation of MnP in tumour compared to muscle regardless of the presence of ascorbate in plasma.

Table I

Metal-centred redox potential for Mn^{III}/Mn^{II} redox couple, $E_{1/2}$ and log k_{cat} for $O_2^{\cdot -}$ dismutation for Mn(III) *N*-alkylpyridylporphyrins.

Porphyrin	$E_{1/2}$/mV vs NHE[a]	log k_{cat}[b]
MnTM-2-PyP^{5+}	+220	7.79
MnTE-2-PyP^{5+}	+228	7.76
MnTnPr-2-PyP^{5+}	+238	7.38
MnTnBu-2-PyP^{5+}	+254	7.25
MnTnHex-2-PyP^{5+}	+314	7.48
MnTnHep-2-PyP^{5+}	+342	7.65
MnTnOct-2-PyP^{5+}	+367	7.71
MnTM-3-PyP^{5+}	+52	6.61
MnTE-3-PyP^{5+}	+54	6.65
MnTnPr-3-PyP^{5+}	+62	6.69
MnTnBu-3-PyP^{5+}	+64	6.69
MnTnHex-3-PyP^{5+}	+66	6.64

[a] The k_{cat} was determined by cyt *c* assay in 0.05 M phosphate buffer, pH 7.8 at 25 ± 1°C [1,2].

[b] The $E_{1/2}$ was determined in 0.05 M phosphate buffer, 0.1 M NaCl, pH 7.8 at 25 ± 1°C.

Table II

Lipophilicity of the series of *ortho* and *meta* isomeric Mn(III)- and reduced Mn(II) *N*-alkylpyridylporphyrins, measured by chromatographic retention factor (R_f) and by their partition between n-octanol and water, log P_{OW}.

Porphyrin	R_f ($Mn^{III}P$)	log P_{OW}($Mn^{III}P$)	Porphyrin	R_f ($Mn^{II}P$)	log P_{OW}($Mn^{II}P$)	log P_{OW}($Mn^{III}P$) − log P_{OW}($Mn^{II}P$)
Mn^{III}TE-2-PyP^{5+}	0.060	−6.70[a]	Mn^{II}TE-2-PyP^{4+}	0.225	−4.69[a]	2.01
Mn^{III}TnPr-2-PyP^{5+}	0.110	−6.09[a]	Mn^{II}TnPr-2-PyP^{4+}	0.340	−3.29[a]	2.80
Mn^{III}TnBu-2-PyP^{5+}	0.190	−5.11[b]	Mn^{II}TnBu-2-PyP^{4+}	0.431	−2.18[a]	2.93
Mn^{III}TnHex-2-PyP^{5+}	0.380	−2.76[b]	Mn^{II}TnHex-2-PyP^{4+}	0.550	−0.73[a]	2.03
Mn^{III}TnHep-2-PyP^{5+}	0.460	−2.10[b]	Mn^{II}TnHep-2-PyP^{4+}	0.578	−0.39[a]	1.71
Mn^{III}TnOct-2-PyP^{5+}	0.490	−1.24[b]	Mn^{II}TnOct-2-PyP^{4+}	0.583	−0.33[a]	0.91
Mn^{III}TM-3-PyP^{5+}	0.050	−6.68[c]	Mn^{II}TM-3-PyP^{4+}	0.125	−6.02[c]	0.66
Mn^{III}TE-3-PyP^{5+}	0.100	−6.24[c]	Mn^{II}TE-3-PyP^{4+}	0.214	−5.24[c]	1.00
Mn^{III}TnPr-3-PyP^{5+}	0.220	−5.00[b]	Mn^{II}TnPr-3-PyP^{4+}	0.381	−3.77[c]	1.23
Mn^{III}TnBu-3-PyP^{5+}	0.400	−4.03[b]	Mn^{II}TnBu-3-PyP^{4+}	0.548	−2.31[c]	1.72
Mn^{III}TnHex-3-PyP^{5+}	0.550	−2.06[b]	Mn^{II}TnHex-3-PyP^{4+}	0.613	−1.74[c]	0.32

R_f values were obtained by TLC on plastic-backed silica gel plates in KNO_3-saturated H_2O:H_2O:acetonitrile = 1:1:8.

[a] Calculated according to equation: log P_{OW} = 12.18 · R_f − 7.43 [26]. The values are similar to those calculated from log P_{OW} vs nC [25]; the deviations are higher with methyl and ethyl analogues.

[b] Determined in water/n-butanol system and converted to water/n-octanol system using equation: log P_{OW} = 1.55 (log P_{BW}) − 0.54 [45].

[c] Calculated according to equation: log P_{OW} = 8.78 · R_f − 7.12.

Table III

Levels of MnTnHex-2-PyP^{5+} in mouse tumour and muscle expressed in μM in tissue determined by LC/ESI-MS/MS method. Tumours and muscle tissues were collected in a 4T1 mouse breast tumour study. Tumours were grown in Balb/c mice (n = 15). Mice were injected twice daily with MnP and ascorbate for 2 weeks from the moment the tumour size reached ~100–200 mm^3, until its volume increased ~5-fold.

PyP^{5+}	MnTnHex-2-PyP^{5+}/ μM in tissue (mean)	SD	Range
Tumor (MnP)	1.65	1.29	0.735 – 5.89
Muscle (MnP)	0.31	0.07	0.166 – 0.417
Tumour (MnP + asc)	2.20	0.84	1.01 – 3.81
Muscle (MnP + asc)	0.48	0.16	0.231 – 0.849